Atmos. Chem. Phys. Discuss., 10, 18731–18780, 2010
www.atmos-chem-phys-discuss.net/10/18731/2010/
doi:10.5194/acpd-10-18731-2010

Atmospheric Chemistry and Physics Discussions

Aerosol ageing in an urban plume – implications for climate and health

P. Roldin[1], E. Swietlicki[1], A. Massling[1,*], A. Kristensson[1], J. Löndahl[1], A. Eriksson[1,2], J. Pagels[2], and S. Gustafsson[3]

[1]Division of Nuclear Physics, Lund University, 221 00, Lund, Sweden
[2]Division of Ergonomics and Aerosol Technology, Lund University, Sweden
[3]Environmental Department, City of Malmö, Sweden
[*]now at: National Environmental Research Institute, Dept. of Atmospheric Environment, Aarhus University, Denmark

Received: 14 July 2010 – Accepted: 18 July 2010 – Published: 10 August 2010

Correspondence to: P. Roldin (pontus.roldin@nuclear.lu.se)

Published by Copernicus Publications on behalf of the European Geosciences Union.

Abstract

The climate and health effects downwind of an urban area resulting from gaseous and particulate emissions within the city are as yet inadequately quantified. The aim of this work was to estimate these effects for Malmö city in Southern Sweden (population 280 000). The chemical and physical particle properties were simulated with a model for Aerosol Dynamics, gas phase CHEMistry and radiative transfer calculations (ADCHEM) following the trajectory movement from upwind Malmö, through the urban background environment and finally tens and hundreds of kilometers downwind Malmö. The model results were validated with measurements of the particle number size distribution and chemical composition. The total particle number concentration 50 km (~3 h) downwind in the center of the Malmö plume is about 3800 cm^{-3} and the Malmö contribution is roughly 35%. Condensation of nitric acid, ammonium and to a smaller extent oxidized organic compounds formed from the emissions in Malmö increases the secondary aerosol formation with a maximum of 0.6–0.7 $\mu g/m^3$ 6 to 18 h downwind of Malmö. The secondary mass contribution dominates over the primary soot contribution from Malmö already 2 to 3 h after the emissions and gives an enhanced total top of the atmosphere direct or indirect aerosol shortwave radiative forcing in the center of the urban plume ranging from −0.3 to −2.3 $W\,m^{-2}$ depending on the distance from Malmö, and the cloud properties. It also gives an increased respiratory tract deposited mass dose, which increases with the distance downwind Malmö.

1 Introduction

In recent years several studies have shown that anthropogenic emissions of trace gases and aerosol particles from urban areas are important for particle properties relevant for climate and population health, not only within the source region itself but also several hundred kilometers downwind (e.g. Seinfeld et al., 2004; Gaydos et al., 2007; Hodzic et al., 2009 and Tie et al., 2009). Hence, there is an urgent need to be able

ACPD
10, 18731–18780, 2010

to accurately incorporate these urban emissions into regional and global three dimensional Chemistry Transport Models (3D-CTMs) and even global climate models. The urban background stations measure freshly emitted particles in the beginning of the ageing process. Still, the distances from the emission sources are much shorter than the spatial scales used in global and regional CTMs (Pierce et al., 2009). Therefore, it is important to study the chemical and physical transformation of particles from urban background scale (0.1–1 km) to CTM grid scale (10–100 km scale).

Several urban plume studies have been carried out within comprehensive but short field campaigns in large cities (>1 million people), e.g. Mexico City (Doran et al., 2007; Hodzic et al., 2009 and Tsimpidi et al., 2010), Tampa (Nolte et al., 2008), Paris (Hodzic et al., 2006) and Copenhagen (Wang et al., 2010), while very few, if any, such studies have been carried out in small to midsize cities (<1 million people). Still, about 60% of the urban population of the world live in small to midsize cities (Population Div. of the Dep. of Economic and Social Affairs of the UN Secretariat), and by number they are far more common and well distributed over the globe than those who live in large cities. Even though one small city's emissions alone are of little concern on a global scale, they together cause a large portion of the global anthropogenic particle and gas phase emissions. Therefore is it important to consider these emissions when discussing climate and health effects of particles and gases on any spatial scale and implement them into regional and global CTMs.

Most previous studies which have approached to model the ageing of urban particle and gas phase emissions downwind urban areas have used Eulerian 3D-CTMs with detailed gas and particle chemistry, but with relatively coarse spatial horizontal resolution (5×5 km–36×36 km) and only very few particle size bins (6–10) (e.g. Hodzic et al., 2006; Gaydos et al., 2007; Nolte et al., 2008 and Hodzic et al., 2009). However, when implementing urban background emissions into CTMs, the spatial resolution should preferably be at least 1×1 km and the size resolved chemical and physical properties relevant for climate and health effects are only poorly represented when using few size bins.

ACPD
10, 18731–18780, 2010

In this work a trajectory model for Aerosol Dynamics, gas phase CHEMistry and radiative transfer calculations (ADCHEM), developed at Lund University (Roldin et al., 2010), has been used to simulate the aging of the urban plume from the city of Malmö in Southern Sweden (13°00′ E, 55°36′ N, 280 000 people) during the year 2005 and 2006. ADCHEM includes all important aerosol dynamic processes, detailed gas and particle phase chemistry and dispersion in the vertical and horizontal direction, perpendicular to the urban plume. The computational advantage of the Lagrangian compared to the Eulerian approach allows the user to include a large number of size bins (in this study 200 size bins between 1.5 and 2500 nm) and still to keep a high horizontal and temporal resolution (in this study 1 km and 1 min). Hence, ADCHEM can be used to model the ageing of urban emissions from urban background to regional or global scales (several hundred kilometers from the source).

This work mainly describes the methods used to estimate the regional influence from the Malmö particle and gas phase emissions, the average results from these urban plume studies and finally gives estimates of different particle properties relevant for climate and population health on the regional scale. For a detailed description and evaluation of ADCHEM the reader is referred to Roldin et al. (2010).

The aim of this study was to estimate the influence of the urban particle and gas phase emissions in Malmö on climate and health relevant particle properties downwind the city (here radiative forcing (ΔF) and respiratory tract deposited dose). A second aim was to test methods and provide results that could form a basis for upscaling from urban sub-grid emissions to the regional scale which can be treated by and implemented in regional and global 3D-CTMs.

2 Methods for urban plume studies

In this section the methods used to characterize the properties of the aerosol particles inside the urban plume from Malmö is described. These methods were applied for 26 urban plume cases and the average and median results are presented in this article.

ACPD
10, 18731–18780, 2010

2.1 Measurements

Particle and gas concentration data from two different stations in Sweden were either used as input data in ADCHEM or to validate the model results. The stations were an urban background station positioned in Malmö (Rådhuset, 55° 36′ N, 13° 00′ E, 30 m a.s.l.) and the European Monitoring and Evaluation Program (EMEP) background station Vavihill (56° 01′ N, 13° 09′ E, 172 m a.s.l.), about 50 km north from Malmö (Fig. 1). Description of the measurement station Vavihill can be found in Kristensson et al. (2008).

The particle number size distributions in Malmö and Vavihill were measured with a Scanning Mobility Particle Sizer (SMPS) and a Twin Differential Mobility Particle Sizer (TDMPS), respectively. The SMPS system in Malmö measured the urban background particle number size distribution at the roof top level of the town hall (Rådhuset) in the north-western part downtown Malmö (Fig. 1). During southerly air masses the station detected particle concentrations which are representative of the major particle emissions from Malmö.

The SMPS system in Malmö sampled air through a PM_{10} inlet (Rupprecht and Patashnik, 1995). The sampled particles were brought to charge equilibrium using a bipolar charger before size separation in a medium Vienna-type Differential Mobility Analyzer (DMA) (Winklmayr et al., 1991) and subsequent counting by a Condensation Particle Counter (CPC) (model CPC 3760A) (TSI Inc., Shoreview, MN, USA). This way a full size distribution between 10 and 660 nm in diameter is measured within 3 min. The short sampling time enables the instrument to capture the rapidly changing particle concentrations at the urban site.

The TDMPS system at the Vavihill field station measured the rural background particle number size distribution from 3 to 900 nm with 10 min time resolution, in a similar way as the SMPS system in Malmö (Kristensson et al., 2008).

As an independent way of testing the accuracy of the ADCHEM model in describing the aerosol chemical composition, data from Time of Flight Aerosol Mass Spectrometry

ACPD
10, 18731–18780, 2010

(ToF-AMS) measurements at Vavihill were compared with the average model results. The AMS measurements were not conducted at the time of the modeled period but during two campaigns in October 2008 and March 2009 (Eriksson, 2009). The AMS results (in total 40 h of data) are selected for periods with southerly air masses passing over the Malmö region between 1–6 h before they reach Vavihill. According to HYSPLIT model trajectories (Draxler and Rolph, 2003) these air masses have their origin from similar European source regions as the trajectories for the modeled case studies (e.g. Great Britain, Germany, Denmark, Benelux and Poland) (see Fig. 2).

Measured concentrations of NO, NO_2, O_3 and SO_2 at the urban background station in Malmö and in addition O_3 at Vavihill were compared with the modeled gas phase concentrations along the trajectory for each urban plume case. All gas concentrations were averaged to 1 h time resolution data when compared with the model results. NO_2 and NO_x were measured with chemiluminescence technique and SO_2 with UV-fluorescence technique. The total NO_x concentration is detected by first oxidizing all NO to NO_2. At both stations O_3 was measured using the principle of UV-absorption.

Apart from measured particle and gas phase concentrations, measurements of the wind direction from a meteorological mast in Malmö (Heleneholm) were used to verify that the urban plume from Malmö was directed toward Vavihill. The wind direction was measured at 24 m a.g.l. The position of the meteorological mast is displayed in Fig. 1.

2.2 The ADCHEM model

For more detailed information about all the modules and methods (e.g. condensation/evaporation algorithms, SOA formation models and size structure methods) and their influence on the model results the reader is refereed to Roldin et al. (2010).

ADCHEM can be divided into three sub-models:

1. an atmospheric aerosol dynamics and particle chemistry model,
2. a chemical gas phase model,

ACPD
10, 18731–18780, 2010

3. a radiative transfer model.

The aerosol dynamic model is a sectional model which discretizes the particle number size distribution into finite size bins. The particles are assumed to be internally mixed which means that all particles of a certain size have equal composition. The model includes the following processes: condensation, evaporation, dry deposition, Brownian coagulation, wet deposition, in-cloud processing with dissolution of SO_2 and H_2O_2 forming sulfate (S(VI)), primary particle emissions, homogeneous nucleation and dispersion in the vertical (1-D model) and horizontal direction (2-D model) perpendicular to an air mass trajectory. The size distribution changes upon condensation/evaporation and coagulation and are either treated with the full-moving, full-stationary or moving-center structure method, which are all mass and number conserving (e.g. Jacobson, 2005b).

The modeled aerosol particles are composed of sulfate, nitrate, ammonium, sodium, chloride, non water soluble minerals (metal oxides/hydroxides), soot, Primary Organic Aerosol (POA), Anthropogenic and Biogenic Secondary Organic Aerosol (ASOA and BSOA). With ADCHEM the SOA formation can either be modeled using the 2-product model approach (Odum et al., 1996), or using the 2D-VBS method, which apart from saturation concentration (C^*) includes oxygen to carbon ratio (O/C-ratio) as a second dimension (Jimenez et al., 2009).

The condensation and evaporation of H_2SO_4, HNO_3, HCl and NH_3 can either be modeled as uncoupled or coupled processes (e.g. Zhang and Wexler, 2008). One advantage using the approach of coupled condensation is that the mass transfer of acids and bases becomes independent of pH in the particle water phase. The disadvantage is however that this method can only be used if the particles are near acid neutralized (S(VI) in the form of SO_4^{-2}) (Zaveri et al., 2008, Zhang and Wexler, 2008 and Roldin et al., 2010). When using the approach of uncoupled condensation the condensation processes of acids and bases are treated as separate processes which depend on the pH in the particle water phase. Therefore this method can also be used when the aerosol particles are not fully acid neutralized. When considering uncoupled condensation

ACPD
10, 18731–18780, 2010

ADCHEM uses the prediction of non-equilibrium growth (PNG) scheme developed by Jacobson (2005a). In this scheme the dissolution of ammonia is treated as an equilibrium process after the diffusion limited condensation/evaporation of all inorganic acids. This enables the model to take long time steps (minutes) without causing the modeled pH to start oscillating.

The gas phase model considers 119 different chemical reactions between 63 individual species. Daily isoprene and monoterpene emissions were simulated separately with the vegetation model LPJ-GUESS (Smith et al., 2001 and Sitch et al., 2003), in which process-based algorithms of terpenoid emissions were included (Arneth et al., 2007; Schurgers et al., 2009). These natural emissions were corrected for anthropogenic land cover according to Ramankutty et al. (2008).

In the present version of ADCHEM about one third of the non-methane volatile organic carbon (NMVOC) emissions from road traffic are benzene, toluene and xylene (BTX). These light aromatic compounds first react with OH followed by either reaction with NO forming products with low SOA-yields, or with HO_2resulting in products with generally higher SOA-yields (Ng et al., 2007). At high NO_x/HO_2 ratio, which generally is the case in urban environments, most of the oxidation products will react with NO, while at remote regions and in the free troposphere the HO_2-pathway usually dominate. Hence, oxidation of BTX in urban environments generally gives relatively low SOA formation, while moving further away from the source the SOA formation can be considerably higher. Here it is mainly benzene, which is the least reactive of the three compounds, that is left to form SOA (Henze et al., 2008).

The radiative transfer model is used to derive the spectral actinic flux which affects the photochemical reaction rates. This model uses a quadrature two-stream approximation scheme, where the radiative fluxes are approximated with one upward and one downward flux component. This scheme was developed and used by Toon et al. (1989) to calculate the radiative transfer in a vertically inhomogeneous atmosphere with clouds and aerosol particles.

ACPD
10, 18731–18780, 2010

For all simulations carried out in this work the full-stationary method with 200 size bins between 1.5 and 2500 nm was used. The condensation of acids and bases were treated as uncoupled processes and the SOA formation was modeled with 2D-VBS for high and low NO_x conditions according to the parameterization in Roldin et al. (2010). The POA was modeled as semi-volatile (C^* between $10^{-2}$and 10^4µg/m^3) and the intermediate VOC (IVOC) emissions (C^* between 10^4 and 10^6µg/m^3) was assumed to be 1.5 times larger than the anthropogenic POA emissions according to Robinson et al. (2007).

2.3 Model inputs

The meteorological data used for all simulations were downloaded from NOAA Air Resource Laboratory Real-time Environmental Application and Display sYstem (READY) (Rolph, 2003). Along each trajectory data of solar irradiance, mixing height and rain fall intensity with 1 h time resolution was included. For every 3 h along the trajectories, vertical temperature, wind speed and relative humidity profiles were received. The vertical temperature, wind speed and relative humidity data was linearly interpolated to the fixed vertical grid, that was used for the simulations. Linear interpolation of all meteorological data was also carried out to increase the temporal resolution to 1 min, which was the time step used by ADCHEM.

Country specific forest and meadow/pasture area coverage information from Simpson et al. (1999), and emissions of isoprene and monoterpenes from LPJ-GUESS and anthropogenic NMVOCs, NO_x, SO_2, CO, NH_3 and $PM_{2.5}$ emissions were included along the trajectories. For Denmark and Southern Sweden (54° 48′ N to 56° 22′ N) the anthropogenic yearly average emissions along the trajectories were received from the National Environmental Research Institute (NERI) in Denmark and the Environmental Dept., City of Malmö (Gustafsson, 2001) in Sweden, respectively. For Danish road emissions, a spatial resolution of 1×1 km^2 was obtained, based on NERI's traffic database with traffic volumes on all road links in Denmark for the year 2005, together with emission factors from the COPERT IV model applied for 2008. For other (non-

ACPD
10, 18731–18780, 2010

road) sources in Denmark, an emission inventory with 17×17 km^2 spatial resolution was used based on Danish national emission inventories for the year 2007 provided by NERI (emission.dmu.dk). For Southern Sweden, all anthropogenic emissions had a spatial resolution of 1×1 km^2. The southern Swedish emission data base has previously primary been used for epidemiological studies in relation to NO_x and NO_2 exposure (e.g. Chaix et al., 2006 and Stroh et al., 2007) For the rest of Europe the emissions within our study were taken from the EMEP emission database for year 2006 (Vestreng et al., 2006). These emissions have a spatial resolution of 50×50 km^2. The yearly anthropogenic emissions were multiplied with country specific diurnal, weekly and monthly variation factors based on the EMEP emission database. The forest and meadow/pasture data was used to estimate the surface albedo and roughness length.

The measured particle number size distributions were averaged to 30 min values in Malmö and at Vavihill. They were parameterized by fitting 5 modal lognormal distributions to the data using the automatic lognormal fitting algorithm DO-FIT, version 4.20 (Hussein et al., 2005). Because of the lower detection limit of 10 nm for the SMPS system in Malmö, the actual number concentration of the nucleation mode particles in Malmö is uncertain. The particle number size distribution upwind Malmö was estimated from the measured background conditions at Vavihill (see Sect. 2.4) and used as initial condition in the model. Limitations and uncertainties with this method are discussed in Sect. 2.7. The contribution from local emissions in Malmö was derived as the difference between the estimated background size distribution and the measured size distribution in Malmö. These particles mainly originate from road traffic within the city. In Sect. 2.5 a description is given of how these local particle emissions were introduced into the model over Malmö.

The initial (48 h upwind Malmö) $PM_{2.5}$ chemical composition was estimated from the aerosol mass spectrometer (AMS) measurements carried out at several European sites (Jimenez et al., 2009) with 36% organics, 25% sulfate, 17% nitrate, 14% ammonium and 8% soot below 1000 m a.g.l. and changing linearly to the top of the model domain

ACPD
10, 18731–18780, 2010

(2000 m a.g.l.) to 22% organics, 30% sulfate, 25% nitrate, 18% ammonium and 5% soot.

2.4 Background particle properties outside the urban plume

To be able to estimate the contribution of urban emissions to the regional background particle concentration between Malmö and Vavihill, the background without influence of the urban plume has to be approximated. This was achieved by selecting measured particle number size distributions averaged to 30 min values before and after the time of arrival of the urban plume from Malmö, at Vavihill. The background was estimated as the average of these two 30 min averages. This background size distribution was also used to represent, upwind Malmö conditions (see Sect. 2.7). The detailed criteria for the selection of background distributions are

1. The trajectory should not move over Malmö or Copenhagen before they reach Vavihill.
2. At the time for the measurement of the estimated background, the air mass trajectory reaching Vavihill should originate from the same source region, 48 h backward in time, as the trajectory of the Malmö plume.
3. The selected background particle number size distribution should have been measured at a maximum of 6 h before or after the urban plume reached Vavihill.
4. The selected background particle number size distributions before and after the Malmö plume was observed at Vavihill should have similar shape and magnitude.
5. The original particle number size distribution at 10 min time resolution should show only low temporal variability within the averaging period.
6. If several size distributions seemed to obey criteria 1 to 6 equally well, the 30 min of particle number size distribution measured nearest in time before or after the Malmö plume reached Vavihill was selected.

ACPD
10, 18731–18780, 2010

2.5 Spin-up time upwind Malmö

The total run time of each simulation was three days, starting two days before the air mass trajectory reached Malmö and continuing one day downwind Malmö. The first two days of the simulations were used to initialize (equilibrate) the particle and gas phase chemistry. During this time the particle number size distribution was kept fixed, while all other parameters were allowed to change. After the trajectory reached the urban background station in Malmö, the particle number size distribution was also allowed to change.

When the trajectory arrived at the southern border of Malmö, the estimated local emission contribution was included in each grid cell within the boundary layer, according to Eqs. (1) and (2). Equation (1) gives the estimated particle number concentration at the time when the trajectory arrived at the measurement station in Malmö, while Eq. (2) gives the estimated particle number concentration for each time step (i) between the southern border of Malmö (i =1) and the measurement station (i =N), at the north western part of the city.

$$c_N^j(D_p) = c_{\text{backg}}(D_p) + \frac{\sum_{k=1}^{N} E_{\text{NO}_x}^j}{\sum_{k=1}^{N} E_{\text{NO}_x^{\text{center}}} c_{\text{traffic}}(D_p)} \quad (1)$$

$$c_i^j(D_p) = \left(\frac{N-i}{N} c_{i-1}^j(D_p) + \frac{i}{N} c_N^j(D_p) \right) \quad (2)$$

$c(D_p)$ in Eqs. (1) and (2) is the concentration of particles with a diameter equal to D_p. N is the number of time steps which the trajectory travels over Malmö before reaching the measurement station. $c_{\text{backg}}(D_p)$ is the estimated background particle concentration outside Malmö (initial concentration), j is the horizontal grid cell index (1–20), $E_{\text{NO}_x}^j$ is the NO_x emissions factor from road traffic in grid cell j, $E_{\text{NO}_x}^{\text{center}}$ is the NO_x emission

ACPD
10, 18731–18780, 2010

factor from road traffic in the center of the horizontal model domain (j=10 and 11) and i is the time step index which starts at 1 when the air mass reaches the southern border of Malmö and reaches N, when the trajectory arrives at the measurement station. $c_{traffic}(D_p)$ is the estimated local particle contribution from road traffic in the center of the urban plume, which was derived by taking the difference between the measured particle number size distribution in Malmö and the estimated upwind background particle number size distribution (Sect. 2.4). When using Eq. (1) the particle number size distribution at the center of the urban plume within the boundary layer becomes comparable to the measured particle number size distribution in Malmö at that time. The horizontal (west to east) NO_x emission profile (E_{NO_x}) for Malmö was derived from the NO_x emission database from road traffic within Malmö by averaging the horizontal NO_x emission profiles at the western and eastern side of the trajectory, upwind of the measurement station. The NO_x emission profile resembles a Gaussian distribution with a maximum in the center of the urban plume (E_{NOx}^{center}) and with a full width at half maximum of 7 km. Since the NO_x emissions from road traffic in Malmö are largest in the center of the horizontal model domain, the particle concentrations derived in the model are highest at the measurement station and drop towards the estimated background concentrations at the horizontal boundaries.

2.6 When does the urban plume from Malmö influence Vavihill?

Wind direction measurements from the meteorological mast in Malmö together with HYSPLIT trajectories were used for a first selection of days with possible influence from Malmö on the background station Vavihill. In total 39 days were identified between April 2005 and October 2006. From these days 232 case studies were selected, to cover all periods with possible influence from Malmö on Vavihill. All these cases were then modeled using a simplified 1-D version of ADCHEM, excluding detailed particle and gas phase chemistry. The modeled particle number size distributions at Vavihill were compared with the measured particle number size distributions at Vavihill at the time of arrival of the trajectories. For those cases, with less than 10% difference between the

ACPD
10, 18731–18780, 2010

measured and modeled number, surface area and volume concentration between 10 and 660 nm in diameter and comparable shape of the measured and modeled particle number size distributions, it was considered to be very likely that the Malmö emissions influenced Vavihill. From these simulations, 26 cases from 26 different days were finally selected. For several days more than one case study satisfied the above mentioned criteria for the agreement between the modeled and measured particle concentrations at Vavihill. Still only one case was selected for each day to ensure that certain conditions were not over represented, when deriving the properties of the urban plume. Table 1 gives the diurnal, weekly and monthly distribution of all 26 case studies. Due to a lack of parallel measurements at Vavihill and Malmö station, no urban plume studies for the period November to March could be carried out.

2.7 The upwind background size distributions

The background contribution to the particle number size distribution in Malmö and upwind Malmö was approximated with the measured Vavihill background size distribution as described in Sect. 2.4. This relies on the premise that the size distribution for the background is not changing between upwind Malmö and Vavihill which are 50 km apart. However, the distributions are not identical at these sites in reality due to aerosol dynamic processes. To illustrate this, the modeled background particle number size distribution outside the urban plume at Vavihill can be compared with the estimated upwind Malmö size distribution (measured Vavihill background particle number size distribution) (see Fig. S1 in the online supplementary material). Figure S1 shows that the size distributions is altered during air mass transport between upwind Malmö and Vavihill for the average of the 26 model cases described in Sect. 2.6. On the other hand, the second message from this exercise is that this change is relatively small (about 200 cm^{-3} or 8% lower particle number concentration between 5 and 1000 nm, outside the urban plume at Vavihill compared with upwind Malmö), and hence can be considered acceptable for the model experiments.

ACPD
10, 18731–18780, 2010

2.8 Estimating the secondary aerosol formation within the urban plume

All 26 selected case studies were modeled with and without anthropogenic gas phase emissions in Malmö. The anthropogenic gases considered were NO_x, SO_2, NMVOCs, IVOC emissions estimated from the POA emissions in Malmö and the low-volatile organic compounds characterized as partly evaporating material from the particle phase after dilution in the atmosphere. The difference between the results with or without anthropogenic gas phase emissions in Malmö were then used to estimate the importance of these emissions for the secondary aerosol formation and to answer the question of how this secondary aerosol formation influences the climate and health relevant particle properties downwind the city.

2.9 Climate and health relevant particle properties downwind Malmö

Using the modeled average particle properties within the urban plume downwind Malmö attempts were made to estimate the average impact of Malmö emissions on the regional scale, both for shortwave radiative forcing (ΔF), with and without clouds, as well as health relevant parameters like the deposited dose in the respiratory tract. The radiative forcing and the respiratory tract particle deposition due to the gas phase and particle emissions in Malmö were calculated for different distances (or hours) downwind Malmö.

To be able to estimate the yearly average shortwave radiative forcing from the Malmö emissions, the average particle properties for the 26 case studies were assumed to be representative for the yearly average particle properties in the Malmö urban plume within the boundary layer. From October to March the boundary layer height was assumed to be 300 m during the night reaching a maximum of 500 m during the day, while between April and September it was assumed to be 300 m during the night reaching a maximum of 1200 m during the day. For the investigation of light scattering and absorption of the aerosol particles, the average relative humidity profile from all 26 simulations in Malmö was used, with an average relative humidity of 78% within the lowest 2000 m

ACPD
10, 18731–18780, 2010

of the atmosphere. The particle growth factors due to water uptake were calculated with the thermodynamic model used in ADCHEM. Size-resolved refractive indices of the aerosol particles were estimated from the modeled volume fractions of soot, organic matter, minerals (metal oxides/hydroxides), water soluble inorganic salts and water, with refractive indices reported by Schmid et al. (2006), Horvath (1998) and Sokolik and Toon (1999).

The radiative forcing caused by the emissions in Malmö at the surface and at the top of the atmosphere (TOA) was calculated by taking the difference between the modeled irradiance inside and outside the urban plume. The shortwave radiative forcing of the Malmö particle emissions was calculated for each hour of the day (24 h) of each month of the year and then averaged to get the estimated yearly average shortwave radiative forcing in the urban plume from Malmö.

To be able to estimate the radiative forcing during the presence of clouds an adiabatic cloud parcel model was used to derive realistic cloud properties (Jacobson, 2005b). In the model the updraft velocity inside the clouds was assumed to be 1.0 m/s. Only the inorganic salts were allowed to take up water, while the organic fraction was treated together with minerals and soot as an insoluble core.

In the radiative transfer model 100 m or 500 m thick clouds with the properties modeled with the adiabatic cloud parcel model were included at the top of the boundary layer. The absorption of infrared radiation inside the clouds was not considered in the model.

The total deposition particle dose in the respiratory tract was estimated by calculating the deposition fraction of each particle size bin at a respiratory tract relative humidity of 99.5%, according to the procedure described by Löndahl et al. (2008). The deposited fractions of all particle sizes were calculated using the ICRP model for adult men and women during light exercise (ICRP, 1995). The deposited number, surface area and mass dose was calculated as a function of total deposited fraction (TDF), concentration (C), exposure time (t) and inhaled volume per unit time (Q). The deposited dose was

ACPD
10, 18731–18780, 2010

calculated with Eq. (3), assuming Q to be 1.0 $m^3 h^{-1}$.

$$\text{Dose} = \text{TDF} \cdot C \cdot t \cdot Q \quad (3)$$

3 Results and discussion

The influence of Malmö city emissions on rural background particle concentrations is studied in 26 different cases using HYSPLIT air mass trajectories starting upwind Malmö, going over Malmö and stretching hundreds of kilometers downwind of Malmö (Fig. 2). Most of the simulated trajectories originate over continental Europe (e.g. Germany, Poland and Benelux) or Great Britain. The trajectories pass over the EMEP background station Vavihill, ca. 50 km downwind and north of Malmö. Vavihill is used for the validation of aerosol properties modeled with ADCHEM. Downwind Vavihill, the majority of trajectories continue northward over Sweden.

3.1 Modeled and measured particle number size distributions in the urban plume of Malmö

Figure 3 illustrates the modeled average (a) and median (b) particle number size distributions in Malmö and at different distances downwind of Malmö in the center of the urban plume. As a comparison the measured average and median particle number size distributions at Vavihill, with or without influence from Malmö are also displayed. The shape of the size distribution 50 km downwind of Malmö from modeling and from measurements at Vavihill is identical in the urban plume and the total number concentration agrees to within 3% and 1% for the average and median, respectively. This indicates that the modeled particle number size distributions in the urban plume between Malmö and Vavihill are realistic. The relatively large concentration (~3000 cm^{-3}) in the nucleation mode for the average particle number size distribution in Malmö is due to two daytime cases when the nucleation mode in Malmö was clearly dominating the total number concentration. These particles have a relatively short lifetime (minutes to

ACPD
10, 18731–18780, 2010

hours) because of coagulation and dry deposition processes downwind Malmö. However, a small fraction (~10%) of these particles survives in the atmosphere all the way to Vavihill, where they appear as a mode around 18 nm in diameter. The lognormal parameterizations of the modeled size distributions in Fig. 4a and b, derived with the DO-FIT algorithm, are given in Table S1 and S2 in the online supplementary material, respectively.

Figure 4 shows the modeled average particle number size distributions at the time of arrival at Vavihill at different distances from the center of the urban plume (perpendicular to the air mass trajectory). The results illustrate that for a compact and homogeneously populated city like Malmö the urban influence on the particle properties 50 km downwind the city decreases steeply from the urban plume center towards the urban plume boundaries with only marginal influence more than 6 km outside the center of the urban plume.

By subtracting the modeled background particle number size distribution outside the urban plume (9 km from the center of the urban plume) from the modeled distributions inside the plume, the urban emission contribution in the center of the urban plume was estimated at different distances downwind Malmö (see Fig. 5). As a validation of the model results the urban contribution at Vavihill (50 km downwind Malmö) was also derived directly from the measured size distributions inside and outside the urban plume. Within Malmö city and close to Malmö the emissions have a large influence on the nucleation and Aitken mode particle concentration. However, most of the nucleation mode particles formed in Malmö are lost by coagulation and dry deposition before the urban plume reaches Vavihill. The soot mode particles mostly from traffic, indicated at about 50 nm in Malmö, grew because of condensation to about 65 nm, 50 km downwind the city. As will be shown in Sect. 3.4 this condensational growth is important for these particles' ability to form cloud droplet. Table 2 shows the urban contribution to the average and median number, surface area and volume concentrations for particles between 5 and 1000 nm in diameter at different distances downwind Malmö, in the center of the urban plume. The total particle number concentration decreases rapidly downwind

ACPD
10, 18731–18780, 2010

Malmö, mainly due to coagulation of the freshly emitted particles onto the long distance transported accumulation mode particles. The estimated Malmö city average contribution to the urban background number concentrations is 61% or 4247 cm^{-3} in absolute terms. At Vavihill, 50 km downwind of Malmö, the average Malmö number concentration contribution is 36% (1371 cm^{-3}) according to the model and 34% (1259 cm^{-3}) according to the DMPS measurements. The modeled volume concentration contribution from the emissions in Malmö increases with 45% between Malmö and 50 km downwind the city center (from 1.18 to 1.71 $\mu m^3 m^{-3}$), mainly attributed to the secondary aerosol formation within the urban plume. The last two rows in Table 2 give the estimated average and median number, surface area and volume concentration contribution at Vavihill, derived from the particle number size distribution measurements. The number concentration contribution derived from the model at Vavihill is 9% higher for the average and less than 1% lower for the median concentration contribution than the measurements. For the surface area and volume concentration contribution the model gives 18% and 36% higher average and 25% and 53% higher median value than the measurements at Vavihill, respectively. These discrepancies between the model and the measurements are caused by varying concentrations of particles above 300 nm diameter. These concentration variations are of little importance to the total number concentrations, but have large impact on the volume concentrations.

3.2 Uncertainties of the urban emission contribution downwind Malmö

There are several reasons why the modeled and measured urban concentration contributions are uncertain. Listed are the 2 reasons which are regarded as the most important.

1. The method used to estimate the urban contribution downwind Malmö requires that the measured background particle number size distribution at Vavihill is representative for the background conditions outside the urban plume between Malmö and Vavihill. The criteria for the selection of the background distributions were

ACPD
10, 18731–18780, 2010

therefore designed to fulfill this requirement (see Sect. 2.4). However, since the background distributions at the time of arrival of the urban plume have to be approximated from the measurements a few hours before and after the urban plume influence Vavihill, some uncertainties with the derived background distributions still remain. This is particularly true for single case studies, but the uncertainties decreases when averaging for many cases, as performed in this study. It is hard to quantify the potential error in the estimated background particle number size distributions. However, we believe that the estimated average and median background number concentration are at least within 20% from the correct values. A 20% error in the estimated average background number concentration outside Malmö would cause an error in the estimated urban contribution within the city of only 13%. However, at Vavihill where the difference between the background and urban plume number concentration is smaller the error would become 35%.

2. Another difficulty is the selection of the periods when the urban plume from Malmö affects the background station. In this work, wind direction measurements, HYSPLIT air mass trajectories and aerosol dynamics model simulations, were used to find out when the plume from Malmö influenced the background station at Vavihill. On the one hand, these methods are objective in the sense that they do not introduce any bias in terms of individual opinions on how the size distribution downwind the city "should" look like. On the other hand, these methods are an uncertain way to trace the anthropogenic influence. For better precision, the methods could be complemented with measurements of NO_x or CO at the background station, which could be used as tracers for the urban influence. Unfortunately, these measurements were not available from the station at Vavihill for time periods when this study was carried out.

ACPD
10, 18731–18780, 2010

3.3 Modeled and measured particle and gas phase chemistry

A reasonable agreement between the modeled and the measured gas phase concentrations is important for the modeled particle chemistry. Although the deviation for certain gas phase species is higher than 100% for single case studies, the agreement is better between the average modeled and the measured concentrations as shown in Table 3.

The modeled average ozone concentrations in Malmö is about 20% higher than the measured values, while at Vavihill the model is less than 10% higher than the measurements. Both the measurements and the model give considerably lower ozone levels in Malmö than at Vavihill, with larger differences for the measurements compared to the modeled values.

For NO and NO_2 the modeled concentrations deviate with about 35% and −10% compared to the measured concentrations, respectively. However, the modeled NO_x ($NO+NO_2$) concentration is in almost exact agreement with the measurements. In the model the molecular NO/NO_x emission ratio was set to 0.9 for all NO_x emission sources. This ratio should probably be lower for better agreement between the modeled and the measured NO and NO_2 concentrations in Malmö. The modeled average SO_2 concentration in the surface layer is about 10% lower than the measured concentration

Figure 6 displays the modeled average $PM_{2.5}$ mass fractions of all chemical compounds considered by the model from 6 h upwind Malmö until 24 h downwind Malmö. At Malmö the soot, organics and mineral (metal oxides/hydroxides) mass concentrations increase because of the primary particle emissions in the city. According to the model the organic particle content make up between 22% and 34% of the total $PM_{2.5}$ mass, with a maximum in Malmö and a minimum about 15 h downwind Malmö. The inorganic salt content is dominated by ammonium nitrate, with a nitrate $PM_{2.5}$ mass fraction varying between a minimum of 24% in Malmö to a maximum of 44% 15 h downwind Malmö. As expected, the ammonium concentrations show a clear correlation with the nitrate content. According to the model the PM in the urban plume is fully

ACPD
10, 18731–18780, 2010

or partly neutralized with between 1 and 2 ammonium ions per sulfate ion. To be more precise; with an average ration of 1.85 at 1–2 h upwind Malmö, which decreases to 1.55 at 24 h downwind Malmö.

Figure 7 displays PM_1 mass fraction pie charts and mass size distributions of the modeled and measured chemical compounds which can be detected with ToF-AMS. Overall, the modeled PM_1 mass fractions are almost the same as the measured ones. However, the number of ammonium ions per sulfate and nitrate ion is slightly lower for the modeled values compared to the measurements, which illustrates that the AMS method detected more neutralized aerosol particles than the model. The shape of the modeled mass size distributions agree with the measurements. ADCHEM is able to reproduce the larger mode diameter for the nitrate and ammonium mass size distributions, compared to the organic mass size distribution. However, the measured organic mass size distribution is shifted to even smaller particles compared to the modeled total mass size distribution. In future studies we plan to compare the AMS data inside and outside the urban plume in a similar manner to what was done with the SMPS -data.

The secondary aerosol formation in the surface layer, formed by the anthropogenic gas phase emissions in Malmö, was estimated by taking the difference between the model results with and without anthropogenic gas phase emissions in Malmö (Fig. 8). The total $PM_{2.5}$ mass contribution in the center of the model domain varies from −0.01 to 0.69 µg/m^3 with the maximum between 6 and 18 h downwind Malmö. This secondary aerosol formation is dominated by condensation of nitric acid, which is neutralized by ammonium. The modeled SOA contribution due to the Malmö emissions is small compared to the ammonium nitrate formation but increases in importance with the distance from Malmö, with a maximum of 0.13 µg/m^3 at the end of the model runs 24 h downwind Malmö. The SOA formation will likely continue to increase in importance beyond the spatial and temporal scales studied in this work.

Figure 8 also displays the $PM_{2.5}$ soot contribution from the primary particle emissions in Malmö. The freshly emitted soot particles which are porous soot agglomerates were assumed to have an effective density of 700 kg/m^3 when determining the mass emis-

ACPD
10, 18731–18780, 2010

sions. This effective density agrees with measured values for diesel exhaust particles, between 100 and 150 nm in diameter (Park et al., 2003). The $PM_{2.5}$ mass contribution from the soot particle emissions in Malmö decreases downwind Malmö and more than 2 h downwind the city the secondary aerosol mass formed from the gas phase emissions in Malmö exceeds the $PM_{2.5}$ mass contribution from soot.

3.4 Shortwave radiative forcing of the Malmö emissions

The 3D-bar charts in Fig. 9 display modeled cloud properties 250 m above the cloud base, at different distances (or hours) downwind Malmö for different distances (0–9 km) from the center of the urban plume. The cloud formation was modeled using an adiabatic cloud parcel model described in Sect. 2.9. In Fig. 9a the total number of cloud droplets is shown, while Fig. 9b displays the number of droplets formed because of the emissions in Malmö. Initially downtown Malmö the number of cloud droplets formed from the primary particle emissions is 56 cm^{-3} (6%) higher in the center of the urban plume compared to the background, while 40 km downwind Malmö the number of droplets reaches a maximum of 127 cm^{-3} (12%) higher at the center of the urban plume compared to the background. The increasing influence of the urban emissions on the number of cloud droplets from Malmö until 40 km downwind Malmö are mainly due to the secondary nitrate formation. More than 40 km downwind Malmö the modeled cloud droplet contribution due to the emissions in Malmö decreases continuously, reaching 30 cm^{-3}(5%), 24 h downwind Malmö.

ADCHEM assumes that all particles are internally mixed, while in reality the freshly emitted soot particles in Malmö will be externally mixed in and at short distances downwind the city. Since these externally mixed soot particles are non-water soluble they will not influence the cloud droplet number (CDN) concentration in Malmö. Therefore the modeled number of cloud droplets formed by the primary particle emissions from Malmö will most likely be overestimates in and near the city. However, more than 30 km downwind the city the amplified CDN concentration within the urban plume are mainly caused by the secondary nitrate formation, and the assumption of treating the soot

ACPD
10, 18731–18780, 2010

particles as internally mixed has less influence on the results.

While the number concentration of cloud droplets is higher inside than outside the urban plume, the total cloud water content is essentially the same. Hence, the geometric mean diameter (GMD) of the cloud droplets decreases with increasing number of droplets (Fig. 9c). The smallest dry particle activation diameter is also changed because of the urban emissions. In the center of the urban plume in the greater Malmö area the smallest diameter of activation is about 15 nm larger compared to the background (Fig. 9d). This is attributed to the lower water uptake of the freshly emitted primary particles in Malmö compared to the background, but also due to a lower maximum supersaturation in the more polluted clouds.

The 3D-bar charts in Fig. 10 show the calculated anthropogenic shortwave radiative forcing due to the Malmö emissions at the TOA without (a) and with (b) 100 m thick clouds being present at different distances (or hours) downwind Malmö and for different distances (0–9 km) from the center of the urban plume. Figure 10c and d display the radiative forcing only caused by the secondary aerosol (SA) formed from the gas phase emissions in Malmö with and without the 100 m thick clouds. Without clouds the shortwave radiative forcing in the center of the urban plume, decreases with almost 40% from Malmö to 40 km downwind the city (from −0.83 to −0.51 W/m^2), while when 100 m thick clouds being present the radiative forcing is more than doubled from Malmö to 40 km downwind the city (from −1.1 to −2.3 W/m^2). This increase can be explained by the condensation of nitric acid and ammonia between Malmö and 40–50 km (~3 h) downwind the city (Figs. 8 and 10d), which significantly amplifies the number of particles which are activated as cloud droplets (Fig. 9b). However, more than 40–50 km downwind Malmö the radiative forcing decreases even when clouds are present. This is because the number of available cloud condensation nuclei (CCN) decreases due to deposition and coagulation. Without clouds the secondary aerosol formation has insignificant influence on the radiative forcing at short distances (~20 km) downwind the city. But between 6 and 18 h downwind Malmö, when the secondary aerosol contribution from Malmö is largest (Fig. 8), the influence becomes more pronounced and

ACPD
10, 18731–18780, 2010

even exceeds the effect from the primary particle emissions in Malmö (Fig. 10a and c).

Table 4 displays the average radiative forcing within the 20 km wide horizontal model domain at the surface and at the TOA, at different distances (or hours) downwind Malmö with 100 m thick clouds, 500 m thick clouds or without clouds being present. At the TOA the shortwave radiative forcing is several times smaller than at the surface, especially without clouds present. This is since the primary soot particles emitted in Malmö absorbs the solar radiation and heat the atmosphere but still prevent the solar irradiance from reaching the surface. If 500 m thick clouds are present instead of 100 m thick clouds the modeled shortwave radiative forcing become about three times smaller both at the surface and at the TOA. This is because for optically thick clouds the aerosol particle (cloud droplet) properties have less influence on the optical properties of the clouds (Twomey, 1977).

It is important to remember that the average particle properties used for the radiative forcing calculations are derived from cases with southerly air masses, which generally originate from relatively polluted regions in Europe. Therefore the number of cloud droplets at the background will likely be higher compared to air masses originated over e.g. the northern part of Sweden. This decreases the estimated climate impact from the emissions in Malmö, especially if the emissions influence the cloud properties. The derived yearly average shortwave radiative forcing could therefore be considered as a lower estimate of the climate impact from the particle and gas phase emissions in Malmö.

3.5 Respiratory tract deposited dose of the Malmö particle emissions

The 3D-bar charts in Fig. 11a–c display the estimated respiratory tract deposited number, surface area and mass dose caused by the emissions in Malmö at different distances from the center of the urban plume and at different distances downwind Malmö, while Fig. 11d gives the deposited mass dose which is caused by the secondary aerosol formation (ammonium nitrate and SOA), due to the gas phase emissions in Malmö.

ACPD
10, 18731–18780, 2010

Table 5 gives the estimated average deposited dose within the 20 km wide horizontal model domain together with the fraction of the total deposited dose, which is caused by the emissions in Malmö at different distances downwind the city. From Fig. 11 and Table 5 it is evident that the deposited number dose decreases rapidly during the transport away from Malmö, with the deposited number dose at Vavihill being less than 50% of the deposited number dose in Malmö. The reason for this is that the concentration of the nucleation mode particles decreases, mainly due to coagulation. However, 24 h downwind Malmö the deposited number dose increases again, which is attributed to homogeneous nucleation.

In Malmö more than 50% of the deposited number dose in the respiratory tract originates from local emissions, while only a few percent of the total surface area and mass dose are due to the emissions within the city. Opposite to the deposited number dose the deposited mass dose from the Malmö emissions increases significantly when moving away from the city (Fig. 11c–d). The explanation for this finding is the condensation of nitric acid, ammonia and SOA onto the primary particles, which apart from increasing the mass concentration, also increases the hygroscopicity of the freshly emitted soot agglomerates and thereby increases the deposition probability of the accumulation mode particles in the respiratory tract. The deposited surface area dose shows a much weaker dependence on distance from Malmö. This is an important observation since particle surface area has been suggested as a relevant dose metric for particle-related adverse health effects.

Together with the wind rose in Fig. S2 in the online supplementary material, Table 5 can be used to estimate the average number, surface area and mass dose of particles originating from Malmö at any point within 50 km from the city center. Due to prevailing wind directions the exposure to the aged particle emissions from Malmö can be considerably higher in certain neighborhoods compared to others. This is particularly the case for people living in a 22.5° wide sector in the direction N to NNE from Malmö, in which the urban plume from Malmö is directed twice as often as the average.

ACPD
10, 18731–18780, 2010

It is today difficult to comment quantitatively on the effects of these particle exposures. For example, it is not clear whether the primary soot and POA emissions are more or less important for human health compared to the SOA and ammonium nitrate. However, the chemically resolved approach used in this study is likely to be very valuable when more detailed knowledge of the causative agents of particle related health effects becomes available.

4 Summary and conclusions

In this work a coupled aerosol dynamics, gas phase chemistry and radiative transfer model (ADCHEM) has been used first, to test if it can correctly model an ageing urban plume, in this case generated by Malmö, a city with 280 000 inhabitants in Southern Sweden. However, the main objective has been to use ADCHEM to estimate the climate and health impacts of the ageing plume.

ADCHEM was able to accurately model the ageing of the particle number size distribution for 26 different case studies between an urban background site in Malmö and the rural site Vavihill, 50 km downwind of Malmö. At Vavihill, the model results were validated with particle number size distribution measurements. The difference between average modeled and measured concentrations of O_3, NO_2 and SO_2 in Malmö was smaller than 20%, while modeled values were 35% higher for NO. Hence, the model is able to capture the main features of the gas phase chemistry in the Malmö plume, which is required to be able to accurately predict the secondary aerosol formation.

The modeled inorganic and organic particle composition is comparable with ToF-AMS measurements at Vavihill. This illustrates that ADCHEM can be used to model realistic size-resolved particle chemical composition in urban plumes, and that the model results can be used to calculate the optical and hygroscopic properties relevant for climate and health effects.

Malmö contributes with about 1300 particles cm^{-3} at Vavihill, where the number concentration is dominated by primary emissions in the nucleation and Aitken mode.

ACPD
10, 18731–18780, 2010

While the primary particle number contribution continuously decreases downwind of the emissions, the contribution to aerosol particle mass from secondary aerosol formation continues to increase up to several hundred kilometers (~12 h) downwind of Malmö. The secondary aerosol formation is dominated by condensation of nitric acid, formed from the NO_x emissions in Malmö. The maximum secondary aerosol contribution from the gas phase emissions in Malmö of between 0.6 and 0.7 μg/m^3 in the urban plume is reached between 6 and 18 h downwind Malmö.

The freshly emitted primary particles in Malmö have little influence on the cloud properties in the greater Malmö area. However, secondary aerosol formation downwind Malmö leads to growth of the freshly emitted primary particles, which gives a more hygroscopic aerosol. This increases their impact on the cloud properties within the urban plume. Hence, the cloud radiative forcing due to the emissions in Malmö is largest about 40 km downwind Malmö and not within or very near the city. The increasing hygroscopicity and mass accumulation of the particles downwind Malmö change their deposition probability in the respiratory tract and explains why the modeled mass dose caused by the emissions in Malmö, is doubled when moving from Malmö to 50 km downwind the city center and why it is 3.5 times larger 24 h downwind Malmö.

Since 60% of the world population lives in cities with less than 1 million people, i.e. of the same size as Malmö, the climate and health impact of these cities need to be addressed. The urban emission contribution downwind the city center estimated from this study should be used for up-scaling of urban sub-grid emissions to regional scales treated by global and regional chemistry transport models and climate models. The results should further be used to estimate how the particle emissions influence adjacent grid cells of these models. However, since the meteorological conditions, emissions sources, and geographical and population extension vary between different cities more detailed studies of different urban regions around the world are needed to better account for their influence on climate and population health on regional and global scales.

ACPD
10, 18731–18780, 2010

Nevertheless, this study has shown that it is not sufficient to account only for aerosol dynamic processes during the transformation of local scale anthropogenic emissions to larger scales of regional and global models. Gas-phase chemistry and secondary aerosol formation are necessary entities to account for during the prediction of lung deposition and climate effects of particles in the ageing urban plume.

Supplementary material related to this article is available online at: http://www.atmos-chem-phys-discuss.net/10/18731/2010/acpd-10-18731-2010-supplement.pdf.

Acknowledgements. This work has been supported by the European Commission 6th Framework program projects: EUCAARI, contract no 036833-2 (EUCAARI) and EUSAAR, contract no 026140 (EUSAAR). We also gratefully acknowledge the support by the Swedish Research Council through project no 2007–4619 and the Strategic Research Program MERGE: Modeling the Regional and Global Earth System. The Swedish Research Council also funded the purchase of the HR-ToF-AMS instrument through Research Equipment Grant no 2006–5940. The DMPS measurements at Vavihill were supported by the Swedish Environmental Protection Agency within the Swedish Environmental Monitoring Program. The support by the Swedish Research Council for Environment, Agricultural Sciences and Spatial Planning (Formas) through project no 2009–615 and 2008–1467 is also gratefully acknowledged.

The authors would also like to thank Almut Arneth and Guy Schurgers at Department of Earth and Ecosystem Sciences, Lund University for the provide BVOC emissions over Europe, Harri Kokkola, Joni-Pekka Pietikäinen and Jussi Malila at Kuopio University, for valuable help during the development of the adiabatic cloud parcel model, Henrik Nilsson at Environmental Dept., City of Malmö for the gas and wind direction measurements in Malmö, Tareq Hussein from Helsinki University for help with the lognormal-fitting of the measured and modeled particle number size distributions and Matthias Ketzel and Fenjuan Wang from Danish National Environmental Research Institute for help with the implementation of the Danish anthropogenic gas and particle phase emissions.

References

Arneth, A., Niinemets, Ü., Pressley, S., Bäck, J., Hari, P., Karl, T., Noe, S., Prentice, I. C., Serça, D., Hickler, T., Wolf, A., and Smith, B.: Process-based estimates of terrestrial ecosystem isoprene emissions: incorporating the effects of a direct CO_2-isoprene interaction, Atmos. Chem. Phys., 7, 31–53, doi:10.5194/acp-7-31-2007, 2007.

Chaix, B., Gustafsson, S., Jerrett, M., Kristersson, H., Lithman, T., Boalt, Å, and Merlo, J.: Children's exposure to nitrogen dioxide in Sweden: investigating environmental injustice in an egalitarian country, J. Epidemiol. Commun. H., 60, 234–241, 2006.

Doran, J. C., Barnard, J. C., Arnott, W. P., Cary, R., Coulter, R., Fast, J. D., Kassianov, E. I., Kleinman, L., Laulainen, N. S., Martin, T., Paredes-Miranda, G., Pekour, M. S., Shaw, W. J., Smith, D. F., Springston, S. R., and Yu, X.-Y.: The T1-T2 study: evolution of aerosol properties downwind of Mexico City, Atmos. Chem. Phys., 7, 1585–1598, doi:10.5194/acp-7-1585-2007, 2007.

Draxler, R. R. and Rolph, G. D.: HYSPLIT (Hybrid Single-Particle Lagrangian Integrated Trajectory) Model access via NOAA ARL READY Wedsite (http://www.arl.noaa.gov/ready/hysplit4.html), NOAA Air Resources Laboratory, Silver Spring, MD, 2003.

Eriksson, A.: Calibration and First Field Deployment of an Aerosol Mass Spectrometer. M. Sc dissertation at Department of Physics and Department of Design Sciences, Lund University, ISRN: LUTMDN/TMAT-5130-SE, 2009.

Gaydos, T. M., Pinder, R., Koo, B., Fahey, K. M., Yarwood, G., and Pandis, S. N.: Development and application of a three-dimensional aerosol chemical transport model, PMCAMx, Atmos. Environ., 41, 2594–2611, 2007.

Gustafsson S. Uppbyggnad och validering av emissionsdatabas avseende luftföroreningar för Skåne med basår. Licentiat Dissertation at National Environmental Research Institute, Lund University, no. 9, 2001.

Henze, D. K., Seinfeld, J. H., Ng, N. L., Kroll, J. H., Fu, T.-M., Jacob, D. J., and Heald, C. L.: Global modeling of secondary organic aerosol formation from aromatic hydrocarbons: high- vs. low-yield pathways, Atmos. Chem. Phys., 8, 2405–2420, doi:10.5194/acp-8-2405-2008, 2008.

Hodzic, A., Vautard, R., Chazette, P., Menut, L., and Bessagnet, B.: Aerosol chemical and optical properties over the Paris area within ESQUIF project, Atmos. Chem. Phys., 6, 3257–3280, doi:10.5194/acp-6-3257-2006, 2006.

ACPD
10, 18731–18780, 2010

Hodzic, A., Jimenez, J. L., Madronich, S., Aiken, A. C., Bessagnet, B., Curci, G., Fast, J., Lamarque, J.-F., Onasch, T. B., Roux, G., Schauer, J. J., Stone, E. A., and Ulbrich, I. M.: Modeling organic aerosols during MILAGRO: importance of biogenic secondary organic aerosols, Atmos. Chem. Phys., 9, 6949–6981, doi:10.5194/acp-9-6949-2009, 2009.

Horvath H. Influence of atmospheric aerosols upon the global radiation balance. In: Harrison, R.M, Van Greiken, R. (Eds.): Atmospheric Particles IUPAC Series on Analytical and Physical Chemistry of Environmental Systems, vol. 5., Wiley, New York, USA, 1998.

Hussein, T., Dal Maso, M., Petaja, T., Koponen, I. K., Paatero, P., Aalto, P. P., Hämeri, K., and Kulmala, M.: Evaluation of an automatic algorith for fitting the particle number size distributions, Boreal Environ. Res., 10, 337–355, 2005.

ICRP: Human respiratory tract model for radiological protection. ICRP publication 66, International Comission on Radiological Protection. Oxford: Elsevier Science, 1995.

Jacobson, M. Z.: A Solution to the Problem of Nonequilibrium Acid/Base Gas-Particle Transfer at Long Time Step. Aerosol Science and Technology, 39, 92–103, 2005a.

Jacobson, M. Z.: Fundamentals of Atmospheric Modelling (2nd edn.), Cambridge University Press, Cambridge, United Kingdom and New York, NY, USA, ISBN: 0 521 54865 9, 2005b.

Jimenez, J. L., Canagaratna, M. R., Donahue, N. M., Prevot, A. S. H., Zhang, Q., Kroll, J. H., DeCarlo, P. F., Allan, J. D., Coe, H., Ng, N. L., Aiken, A. C., Docherty, K. S., Ulbrich, I. M., Grieshop, A. P., Robinson, A. L., Duplissy, J., Smith, J. D., Wilson, K. R., Lanz, V. A., Hueglin, C., Sun, Y. L., Tian, J., Laaksonen, A., Raatikainen, T., Rautiainen, J., Vaattovaara, P., Ehn, M., Kulmala, M., Tomlinson, J. M., Collins, D. R., Cubison, M. J., Dunlea, E. J., Huffman, J. A., Onasch, T. B., Alfarra, M. R., Williams, P. I., Bower, K., Kondo, Y., Schneider, J., Drewnick, F., Borrmann, S., Weimer, S., Demerjian, K., Salcedo, D., Cottrell, L., Griffin, R., Takami, A., Miyoshi, T., Hatakeyama, S., Shimono, A., Sun, J. Y, Zhang, Y. M., Dzepina, K., Kimmel, J. R., Sueper, D., Jayne, J. T., Herndon, S. C., Trimborn, A. M., Williams, L. R., Wood, E. C., Middlebrook, A. M., Kolb, C. E., Baltensperger, U., and Worsnop, D. R.: Evolution of Organic Aerosols in the Atmosphere, Science, 326, 1525–1529, 2009.

Kristensson, A., Dal Maso, M., Swietlicki, E., Hussein, T., Zhou, J., Kerminen, V.-M., and Kulmala, M.: Characterization of new particle formation events at a background site in Southern Sweden: relation to air mass history, Tellus, 60B, 330–344, 2008.

Löndahl, J., Pagels, J., Boman, C., Swietlicki, E., Massling, A., Rissler, J., Blomberg, A., Sandström, T.: Deposition of Biomass Combustion Aerosol Particles in the Human Respiratory Tract, Inhal. Toxicol., 20, 923–933, 2008.

ACPD
10, 18731–18780, 2010

Ng, N. L., Kroll, J. H., Chan, A. W. H., Chhabra, P. S., Flagan, R. C., and Seinfeld, J. H.: Secondary organic aerosol formation from *m*-xylene, toluene, and benzene, Atmos. Chem. Phys., 7, 3909–3922, doi:10.5194/acp-7-3909-2007, 2007.

Nolte, C. G., Bhave, P. V., Arnold, J. R., Dennis, R. L., Zhang, K. M., and Wexler, A. S.: Modeling urban and regional aerosols-Application of the CMAQ-UCD Aerosol Model to Tampa, a coastal urban site, Atmos. Environ., 42, 3179–3191, 2008.

Odum, J. R., Hoffmann, T., Bowman, F., Collins, D., Flagan, R. C., and Seinfeld, J. H.: Gas/Particle Partitioning and Secondary Organic Aerosol Yields, Environ. Sci. Technol., 30, 2580–2585, 1996.

Park, K., Cao, F., Kittelson, D. B., and McMurry, P. H.: Relationship between Particle Mass and Mobility for Diesel Exhaust Particles, Environ. Sci. Technol., 37, 577–583, 2003.

Pierce, J. R., Theodoritsi, G., Adams, P. J., and Pandis, S. N.: Parameterization of the effect of sub-grid scale aerosol dynamics on aerosol number emission rates, Aerosol Science, 40, 385–393, 2009.

Population Division of the Department of Economic and Social Affairs of the United Nations Secretariat, World Population Prospects: The 2006 Revision and World Urbanization Prospects: The 2007 Revision, http://esa.un.org/unup, last acccess: 7 January 2010, 2010.

Ramankutty, N., Evan, A. T., Monfreda, C., and Foley, J. A.: Farming the planet: 1. Geographic distribution of global agricultural lands in the year 2000, Global Biogeochem. Cy., 22, GB1003, 2008.

Rolph, G. D.: Real-time Environmental Applications and Display sYstem (READY) Website (http://www.arl.noaa.gov/ready/hysplit4.html), NOAA Air Resources Laboratory, Silver Spring, MD, 2003.

Roldin, P., Swietlicki, E., Schurgers, G., Arneth, A., Lehtinen, K. E. J., Boy, M. and Kulmala M.: Development and evaluation of the aerosol dynamic and gas phase chemistry model ADCHEM, Atmos. Chem. Phys. Discuss., 10, 18661-18730, doi:10.5194/acpd-10-18661-2010, 2010.

Seinfeld, J. H., Carmichael, G. R., Arimoto, R., Conant, W. C., Brechtel, F. J., Bates, T. S., Cahill, T. A., Clarke, A. D., Doherty, S. J., Flatau, P. J., Huebert, B. J., Kim, J., Markowicz, K. M., Quinn, P. K., Russell, L. M., Russell, P. B., Shimizu, A., Shinozuka, Y., Song, C. H., Tang, Y., Uno, I., Vogelmann, A. M., Weber, R. J., Woo, J.-H., and Zhang, X. Y.: ACE-ASIA – Regional Climatic and Atmospheric Chemical Effects of Asian Dust and Pollution, B. Am. Meteorol. Soc., 85, 367–380, 2004.

ACPD
10, 18731–18780, 2010

Schmid, O., Chand, D., Karg, E., Guyon, P., Frank, G. P., Swietlicki, E., and Andreae, M. O.: Derivation of the Density and Refractive Index of Organic Matter and Elemental Carbon from Closure between Physical and Chemical Aerosol Properties, Environ. Sci. Technol., 43, 1166–1172, 2009.

Schurgers, G., Arneth, A., Holzinger, R., and Goldstein, A. H.: Process-based modelling of biogenic monoterpene emissions combining production and release from storage, Atmos. Chem. Phys., 9, 3409–3423, doi:10.5194/acp-9-3409-2009, 2009.

Simpson, D., Winiwarter, W., Börjesson, G., Cinderby, S., Ferreiro, A., Guenther, A., Hewitt, N., Janson, R., Khalil, M. A. K., Owen, S., Pierce, T. E., Puxbaum, H., Shearer, M., Skiba, U., Steinbrecher, R., Tarrasón, L., and Öquist, M. G.: Inventorying emissions from nature in Europe, J. Geophys. Res., 104, 8113–8152, 1999.

Sitch, S., Smith, B., Prentice, I., Arneth, A., Bondeau, A., Cramer, W., Kaplan, J., Levis, S., Lucht, W., Sykes, M., Thonicke, K., and Venevsky, S.: Evaluation of ecosystem dynamics, plant geography and terrestrial carbon cycling in the LPJ Dynamic Global Vegetation Model, Glob. Change Biol., 9, 161–185, 2003.

Smith, B., Prentice, I. C., and Sykes, M. T.: Representation of vegetation dynamics in the modeling of terrestrial ecosystems: comparing two contrasting approaches within European climate space, Global Ecol. Biogeogr., 10, 621–637, 2001.

Sokolik, I. N. and Toon, O. B.: Incorporation of mineralogical composition into models of radiative properties of mineral aerosol from UV to IR wavelength, J. Geophys. Res., 104, 9423–9444, 1999.

Steinbrecher, R., Smiatek, G., Köble, R., Seufert, G., Theloke, J., Hauff, K., Ciccioli, P., Vautard, R., and Curci, G.: Intra- and inter-annual variability of VOC emissions from natural and semi-natural vegetation in Europe and neighbouring countries, Atmos. Environ., 43, 1380–1391, 2009

Stroh, E., Harrie, L., and Gustafsson, S.: A study of spatial resolution in pollution exposure modeling, Int. J. Health Geogr., 6, 1–13, 2007.

Tie, X., Madronich, S., Li, G., Ying, Z., Weinheimer, A., Apel, E., and Campos, T.: Simulation of Mexico City plumes during the MIRAGE-Mex field campaign using the WRF-Chem model, Atmos. Chem. Phys., 9, 4621–4638, doi:10.5194/acp-9-4621-2009, 2009.

Toon, O. B., McKay, C. P., Ackerman, T. P., and Santhanam, K.: Rapid Calculation of Radiative Heating Rates and Photodissociation Rates in Inhomogeneous Multiple Scattering Atmospheres, J. Geophys. Res., 94, 16287–16301, 1989.

ACPD
10, 18731–18780, 2010

Tsimpidi, A. P., Karydis, V. A., Zavala, M., Lei, W., Molina, L., Ulbrich, I. M., Jimenez, J. L., and Pandis, S. N.: Evaluation of the volatility basis-set approach for the simulation of organic aerosol formation in the Mexico City metropolitan area, Atmos. Chem. Phys., 10, 525–546, doi:10.5194/acp-10-525-2010, 2010.

Twomey, S.: The Influence of Pollution on the Shortwave Albedo of Clouds, J. Atmos. Sci., 34, 1149–1152, 1977.

Vestreng, V., Rigler, E., Adams, M., Kindbom, K., Pacyna, J. M., van der Gon, D., Reis, H. S., and Traynikov, O.: Inventory review 2006, Emission data reported to LRTAP and NEC Directive, Stage 1, 2 and 3 review and Evaluation of Inventories of HM and POPs. EMEP/MSC-W Technical Report 1/2006 ISSN 1504–6179, available at: http://www.emep.int/, 2006

Wang, F., Roldin, P., Massling, A., Kristensson, A., Swietlicki, E., Fang, D., and Ketzel, M.: Aerosol dynamics in the Copenhagen urban plume during regional transport, Atmos. Chem. Phys. Discuss., 10, 8553–8594, doi:10.5194/acpd-10-8553-2010, 2010.

Winklmayr, W., Reischl, G. P., Lindner, A. O., and Berner, A.: A new electromobility spectrometer for the measurement of aerosol size distributions in the size range from 1 to 1000 nm, J. Aerosol Sci., 22, 289–296, 1991.

ACPD
10, 18731–18780, 2010

Table 1. Diurnal, weekly and monthly distribution of all 26 simulated cases. The time is given as local wintertime at the time when the trajectories arrived in Malmö.

Day	Monday	Tuesday	Wednesday	Thursday	Friday	Saturday	Sunday
No. of sim.	6	2	1	6	1	5	5
Month	Apr	May	Jun	Jul	Aug	Sep	Oct
No. of sim.	1	4	8	3	0	3	7
Time	00:00–06:00		06:00–12:00		12:00–18:00	18:00–00:00	
No. of sim.	7		7		7	5	

ACPD
10, 18731–18780, 2010

Table 2. Estimated average and median particle number, surface area and volume concentration (PN_{tot}, PA_{tot}, and PV_{tot}, respectively) and its contribution from Malmö (PN_{local}, PA_{local}, and PV_{local}) for particles between 5 and 1000 nm in diameter in the center of the urban plume, at different distances downwind Malmö (dw. M.).

Location	PN_{tot}/PN_{local} (cm^{-3})	PA_{tot}/PA_{local} ($\mu m^2 cm^{-3}$)	PV_{tot}/PV_{local} ($\mu m^3 m^{-3}$)
Malmö mean	6940/4247	186.2/42.3	7.35/1.18
Malmö median	4457/2050	151.5/31.2	5.50/0.85
10 km dw. M. mean	5519/2857	182.3/38.2	7.34/1.14
10 km dw. M. median	4002/1624	145.3/25.8	5.30/0.67
20 km dw. M. mean	4824/2247	180.3/36.3	7.44/1.17
20 km dw. M. median	3751/1484	144.4/26.0	5.39/0.70
30 km dw. M. mean	4381/1859	181.5/38.3	7.73/1.43
30 km dw. M. median	3538/1282	149.1/30.9	5.83/1.14
40 km dw. M. mean	4049/1605	181.2/39.2	7.95/1.64
40 km dw. M. median	3334/1159	148.7/32.9	5.97/1.36
50 km dw. M. mean	3793/1371	182.7/38.7	8.13/1.71
50 km dw. M. median	3191/1041	151.0/34.3	6.22/1.47
VVHL mean	3681/1259[a]	175.9/32.9[a]	7.68/1.26[a]
VVHL median	3197/1047[a]	144.2/27.5[a]	5.70/0.96[a]

[a] Derived from the DMPS measurements at Vavihill.

ACPD
10, 18731–18780, 2010

Table 3. Measured and modeled average gas phase concentrations in Malmö and at Vavihill for the 26 model cases.

Species and location	Measured average (ppb)	Modeled average (ppb)
O_3 Malmö	25.7	31.0
O_3 Vavihill	32.4	34.9
NO Malmö	2.8	3.8
NO_2 Malmö	11.2	10.2
SO_2 Malmö	1.1	1.0

ACPD
10, 18731–18780, 2010

Table 4. Average radiative forcing within the 20 km wide model domain at the surface (ΔF_S) and at the TOA (ΔF_{TOA}), with or without clouds, at different distances downwind Malmö.

Position	ΔF_S without clouds (W/m^2)	ΔF_S with 100 m thick clouds (W/m^2)	ΔF_S with 500 m thick clouds (W/m^2)	ΔF_{TOA} without cloud (W/m^2)	ΔF_{TOA} with 100 m thick clouds (W/m^2)	ΔF_{TOA} with 500 m thick clouds (W/m^2)
Malmö	−0.859	−0.610	−0.195	−0.272	−0.296	−0.115
10 km dw. M	−0.823	−0.747	−0.239	−0.239	−0.435	−0.152
20 km dw. M	−0.782	−0.679	−0.220	−0.210	−0.375	−0.137
30 km dw. M	−0.760	−1.035	−0.414	−0.193	−0.737	−0.304
40 km dw. M	−0.752	−1.053	−0.378	−0.186	−0.757	−0.285
50 km dw. M	−0.736	−1.013	−0.334	−0.177	−0.721	−0.258
6 h dw. M.	−0.573	−0.711	−0.262	−0.159	−0.488	−0.187
12 h dw. M.	−0.434	−0.606	−0.228	−0.166	−0.458	−0.173
18 h dw. M.	−0.370	−0.608	−0.245	−0.157	−0.488	−0.194
24 h dw. M.	−0.283	−0.398	−0.154	−0.117	−0.303	−0.128

ACPD
10, 18731–18780, 2010

Table 5. Estimated total deposited number (N), surface area (A) and mass (M) – dose for particles between 3 and 2500 nm in diameter together with the fraction (f) of the deposited dose, which is due to the Malmö particle and gas phase emissions at different locations downwind Malmö. The given values are averages for the 20 km wide horizontal model domain.

Location	N ($h^{-1} \times 10^9$)	A ($mm^2\,h^{-1}$)	M ($\mu g\,h^{-1}$)	$Nf_{Malmö}$	$Af_{Malmö}$	$Mf_{Malmö}$
Malmö	1.655	46.19	4.035	0.560	0.064	0.020
10 km dw. M.	1.304	46.36	4.165	0.437	0.066	0.025
20 km dw. M.	1.158	47.50	4.387	0.338	0.067	0.031
30 km dw. M.	1.023	49.03	4.637	0.330	0.066	0.034
40 km dw. M.	0.940	50.74	4.901	0.292	0.064	0.036
50 km dw. M.	0.890	52.51	5.169	0.260	0.067	0.040
6 h dw. M	0.597	53.27	5.672	0.192	0.062	0.054
12 h dw. M	0.379	49.88	5.832	0.100	0.069	0.068
18 h dw. M	0.303	45.77	5.608	0.0923	0.069	0.070
24 h dw. M	0.495	39.10	4.806	0.228	0.063	0.071

ACPD
10, 18731–18780, 2010

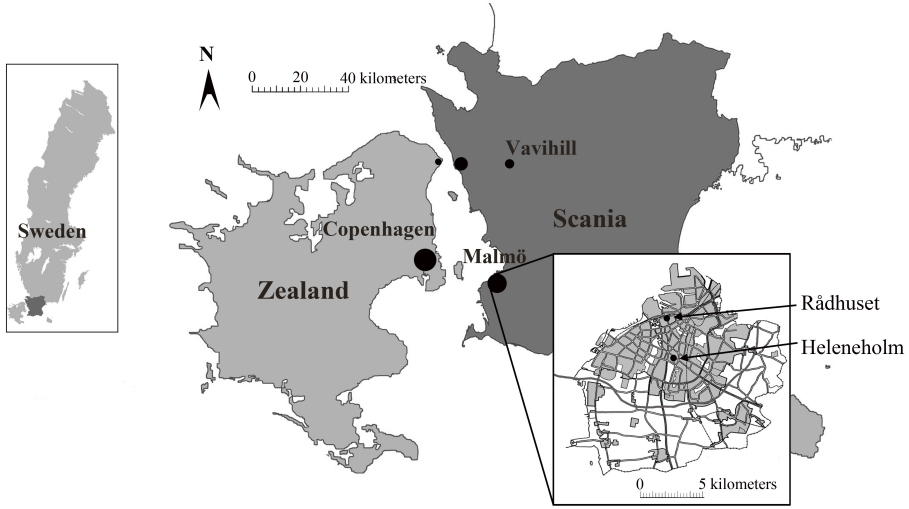

Fig. 1. Geographic map displaying the measurement station in Malmö (Rådhuset), the meterological mast (Heleneholm) and the Vavihill field station in Southern Sweden.

ACPD
10, 18731–18780, 2010

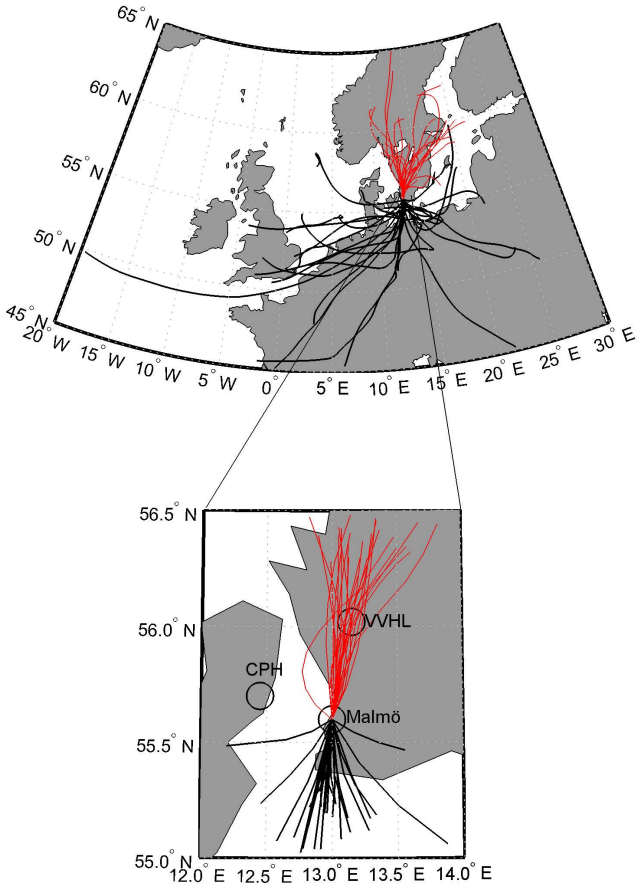

Fig. 2. 24 h forward (red) and 48 h backward (black) trajectories with starting point in Malmö for the 26 selected urban plume cases. Vavihill (VVHL), Malmö and Copenhagen (CPH) are illustrated with circles.

ACPD
10, 18731–18780, 2010

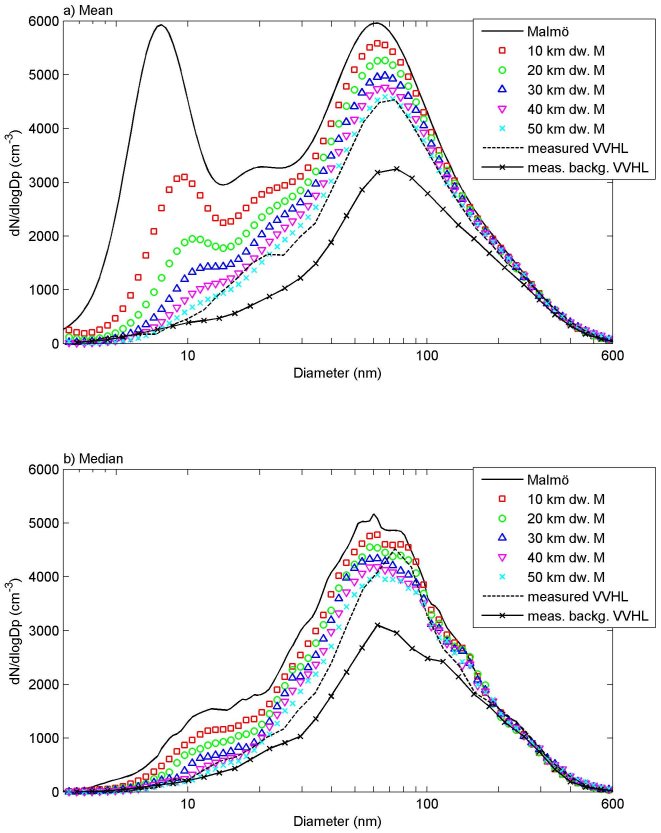

Fig. 3. Modeled average **(a)** and median **(b)** particle number size distributions in the center of the urban plume, 10, 20, 30, 40 and 50 km downwind Malmö, together with the measured (lognormal fitted) particle number size distributions in Malmö and at Vavihill (50 km downwind Malmö). The displayed size distributions in Malmö were derived from the SMPS measurements applying the lognormal fitting algorithm from Hussein et al. (2005) for each individual size distribution and then taking the average and median of these size distributions.

ACPD
10, 18731–18780, 2010

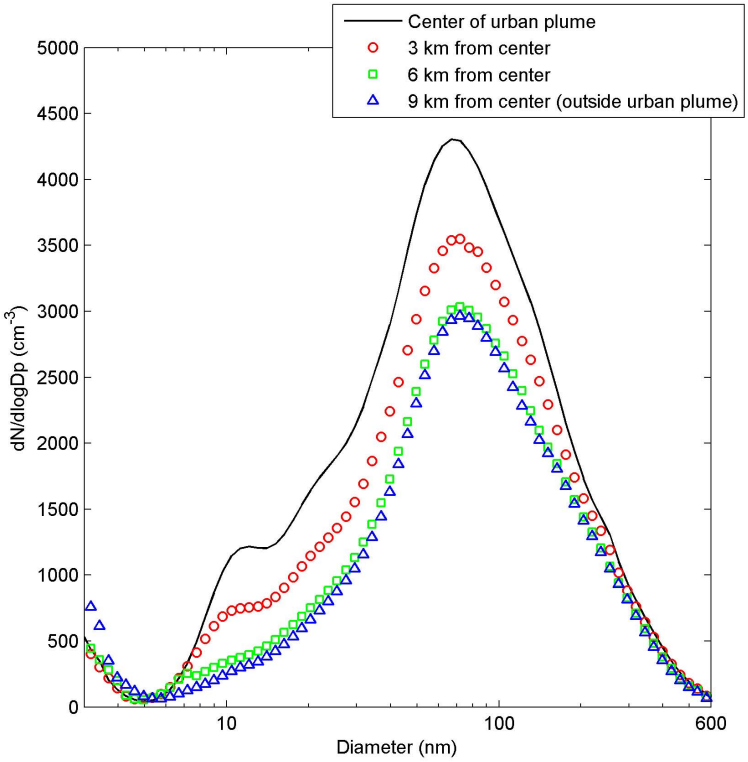

Fig. 4. Modeled average particle number size distributions at different distances (perpendicular to the air mass trajectory) from the center of the urban plume at Vavihill.

ACPD
10, 18731–18780, 2010

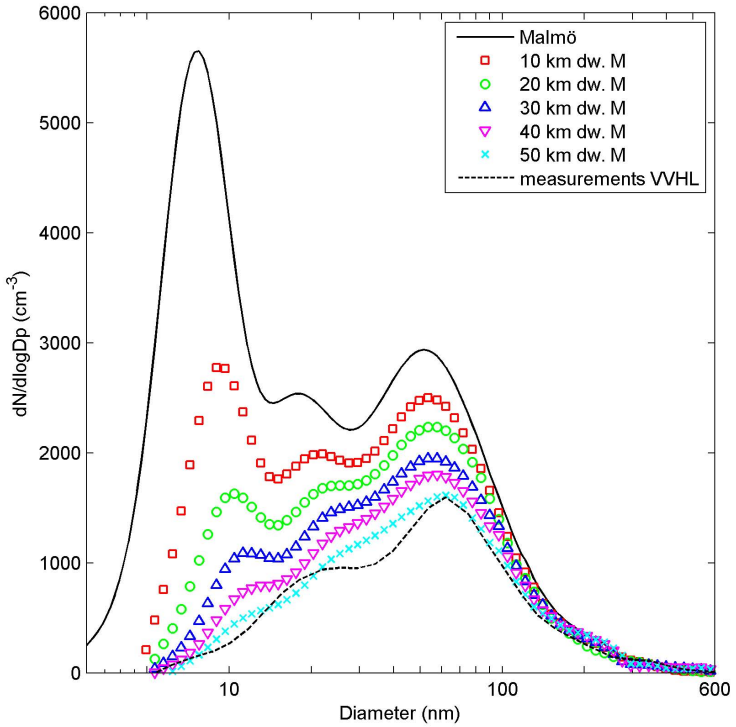

Fig. 5. Estimated average local emission contribution from Malmö, 10, 20, 30, 40 and 50 km downwind Malmö. The particle number size distributions were derived by subtracting the modeled background particle number size distribution from the modeled particle number size distributions within Malmö and at different distances downwind Malmö. The Vavihill distribution is derived by subtracting the measured concentration at Vavihill when the Vavihill station is not influenced by the Malmö plume from the measured concentration at Vavihill when the station is influenced by Malmö.

ACPD
10, 18731–18780, 2010

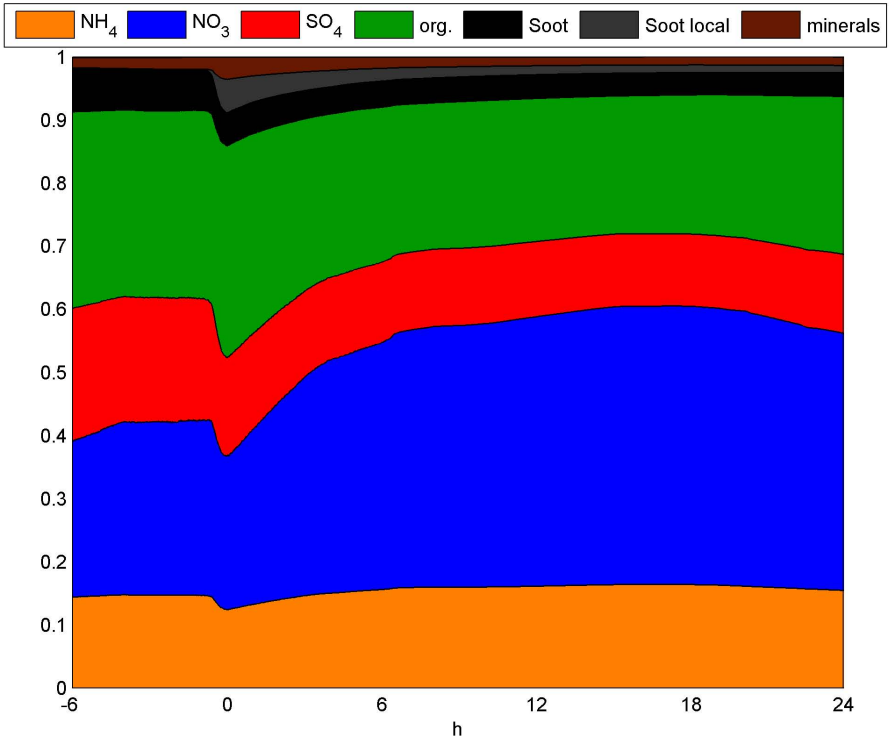

Fig. 6. Modeled average $PM_{2.5}$ mass fractions, 6 h upwind (−6 h) to 24 h downwind Malmö in the surface layer within the urban plume.

ACPD
10, 18731–18780, 2010

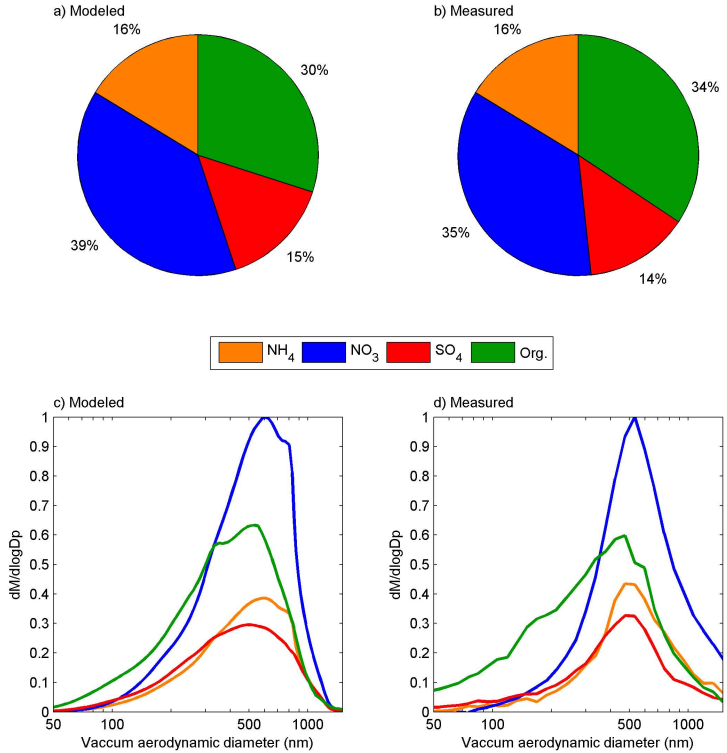

Fig. 7. Modeled **(a)** and **(c)** and measured **(b)** and **(d)** PM_1 mass fractions and mass size distributions of the compounds that can be detected with ToF-AMS. The mass size distributions were normalized with the maximum of the nitrate distributions. The chloride content was very low for the modeled and measured values and is therefore not shown. The model data is the average of the 26 model cases during 2005/2006, while AMS data averages are from the Vavihill October and March campaigns during 2008/2009.

ACPD
10, 18731–18780, 2010

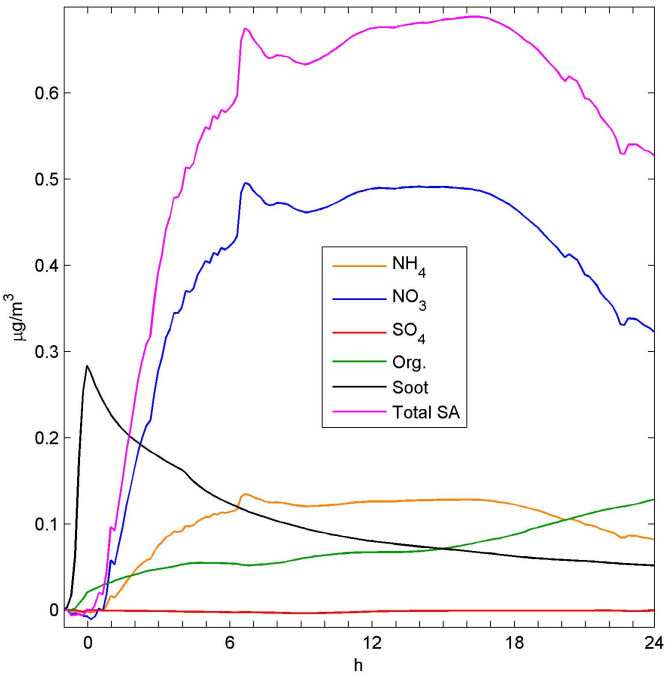

Fig. 8. Modeled average secondary aerosol (SA) formation and primary soot contribution to $PM_{2.5}$, due to gas phase and particle emissions in Malmö in the surface layer downwind Malmö. The effective density of the soot particle emissions over Malmö was estimated to be 700 kg/m^3. The organic contribution only takes into account the condensable organic compounds (SOA) in and downwind Malmö.

ACPD
10, 18731–18780, 2010

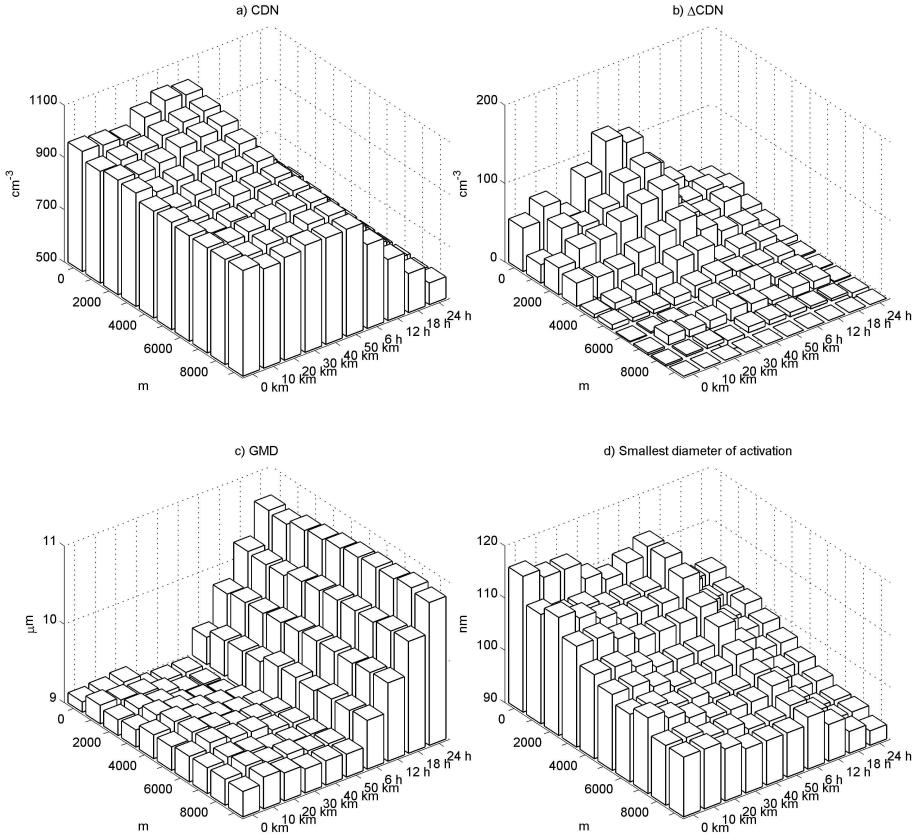

Fig. 9. Modeled cloud properties 250 m above the cloud base, at different distances from the center of the urban plume (0–10 km) and different distances (or hours) downwind Malmö for **(a)** total Cloud Droplets Number (CDN) concentration, **(b)** number of extra cloud droplets due to the gas and particle emissions in Malmö, **(c)** GMD for the cloud droplet distribution and **(d)** the dry diameter of the smallest particles that are activated.

ACPD
10, 18731–18780, 2010

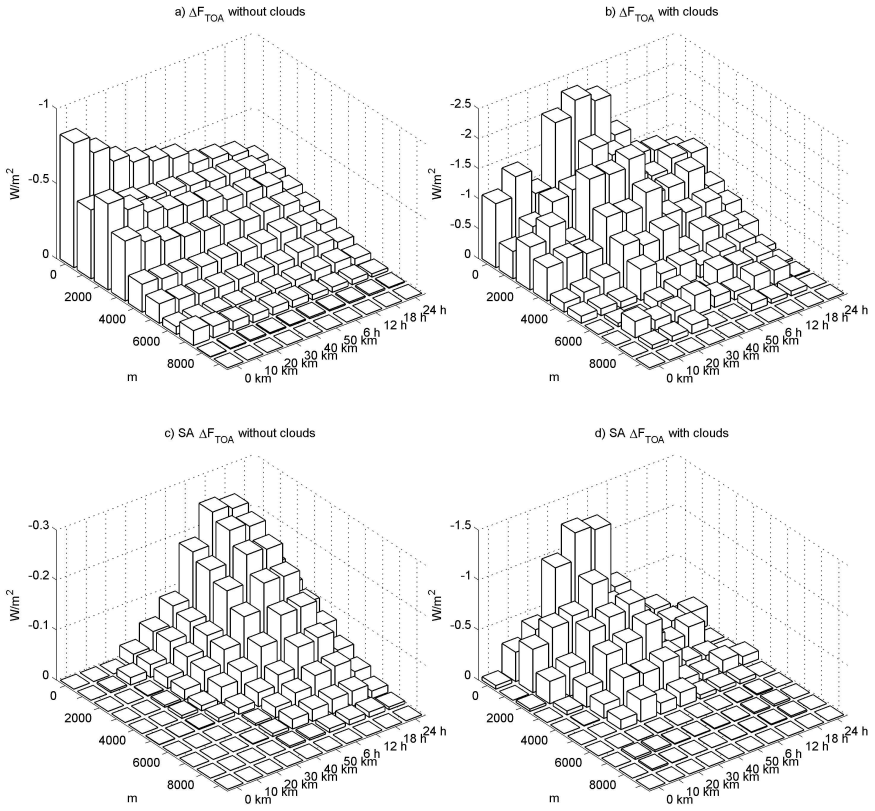

Fig. 10. Modeled anthropogenic shortwave radiative forcing due to Malmö emissions at the top of the atmosphere (TOA) at different distances (or hours) downwind Malmö and at different distances from the center of the urban plume for **(a)** conditions without clouds, **(b)** conditions with 100 m thick clouds at low altitude, **(c)** radiative forcing due to secondary aerosol (SA) formation from Malmö gas phase emissions for conditions without clouds and **(d)** same as **(c)** but with 100 m thick clouds.

ACPD
10, 18731–18780, 2010

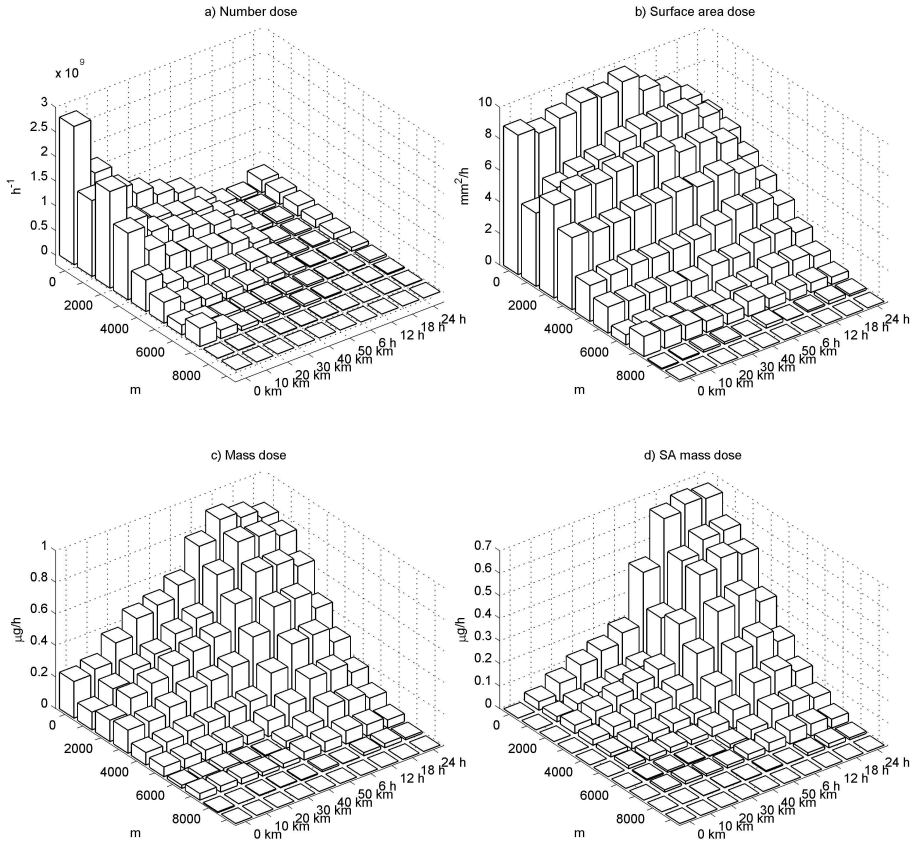

Fig. 11. Modeled respiratory tract deposited particle **(a)** number, **(b)** surface area and **(c)** mass ($PM_{2.5}$) dose originating from the emissions in Malmö. **(d)** shows the mass dose, due to the secondary aerosol formation from the gas phase emissions in Malmö.

ACPD
10, 18731–18780, 2010